

## 8.2 Experimental Research on Pre-chamber Jet Ignition in Rapid Compression Machine and Natural Gas Engine

---

Boyuan Wang, Zhi Wang

### Abstract

Pre-chamber jet ignition is a promising technology for spark ignition engines. In this paper, classical pre-chamber jet ignition and a new pre-chamber jet ignition method named flame accelerated ignition are investigated.

Utilizing the connecting nozzles to generate the jets is the classical form of pre-chamber jet ignition. Two combustion modes were found by the RCM experiments with optical method: double stage combustion and single stage combustion. Double stage combustion mode takes place in the condition with relatively small nozzle dimension, showing long ignition delay and extremely short combustion duration. The jets cannot ignite the mixture directly. Instead, ignition happens at a central position in the main chamber after a lag time followed by the rapid development of the flame with similar speed in each direction. However, the double stage combustion mode has poor combustion stability due to the high randomness of the ignition process inside the main chamber. With single stage combustion mode, the ignition delay and the combustion duration can be shortened simultaneously with satisfying combustion stability. The combustion processes inside the pre-chamber and the main chamber take place continuously. The flame jet develops from the nozzle, composed of thin fire near the nozzle and approximately conical fire in the tip. The speed of flame jet exceeds 15 times than that of conventional flame propagation.

According to the concept of pre-chamber jet ignition and the phenomenon of flame acceleration in tunnel, a new ignition method named flame accelerated ignition (FAI) is proposed. The flame acceleration tunnel can be regarded as a pre-chamber, where flame acceleration happens. Then the combustion in the main-chamber can be induced by the flame jet rushed out of the tunnel. The RCM experiments indicated that the combustion could be evidently enhanced by FAI. The flame jet maintains nearly cylindrical with favorable speed characteristic. Higher indicated thermal efficiency is gained by applying FAI compared to conventional spark ignition in the natural gas engine. In addition, introducing residual gas cavity into the flame acceleration tunnel could expand the misfire limit and improve the defect of FAI mode in lean-burn conditions.

## 1 Introduction

Spark ignition (SI) engines are widely used as automotive power. However, the thermal efficiency of conventional SI engines is not comparable to that of compression ignition engines due to its relatively low combustion velocity, resulting from the combustion mode composed of single-point ignition and flame propagation. Due to increasingly stringent regulations in automotive fuel economy, the combustion process of SI engines needs to be further optimized to gain higher thermal efficiency.

Pre-chamber jet ignition is proposed as a potential approach to improve the performance of SI engines. In this mode, a pre-chamber is introduced into the combustion chamber with spark plug set inside. The pre-chamber serves as an ignition source for the main chamber, providing flame jets spatially distributed inside the main chamber. Meanwhile, the turbulent intensity in the combustion chamber is evidently enhanced. As a result, the combustion velocity is increased, providing the capacity to improve the thermal efficiency [1].

### 1.1 Classical pre-chamber jet ignition

In order to differentiate from the undermentioned new pre-chamber jet ignition method, in this paper, the extensively studied ignition method which utilizes the connecting nozzles to generate the jets is called classical pre-chamber jet ignition.

Classical pre-chamber jet ignition has a long history of development and investigation. Recent years, it has become a hot research topic with the characteristics of relatively small pre-chamber volume and multiple connecting nozzles. The effects of accelerating combustion process has been proved in the engine tests [2-3]. Benefiting from the accelerated combustion velocity, the compression ratio of SI engines with pre-chamber jet ignition system could be increased by 2~3 due to the expanded knock limit [4-5].

To further explore the potential of pre-chamber jet ignition, auxiliary fuel system is introduced into the pre-chamber in order to form a rich mixture condition inside. In this case, the jet could ignite extremely lean mixture ( $\lambda=2.1$  for gasoline engine [6] and  $\lambda=2.9$  for natural gas engine [7]) in the main chamber, leading to higher thermal efficiency.

Although it is proved that the performance of SI engines could be improved by using pre-chamber jet ignition, the combustion process is the result of comprehensive effects of thermal effect, chemical reaction and turbulent flow, which is rather complicated. In order to investigate the mechanism of pre-chamber jet ignition, fundamental researches based on optical and numerical methods have been conducted to investigate the structure of flame and jet [8-9], effects of pre-chamber geometric conditions [10-11], and detailed process of combustion and flow [12-14] in recent years. However, considering the complexity of pre-chamber jet ignition, it still needs to be further recognized.

In this paper, Different pre-chamber nozzle configurations were investigated on rapid compression machine with full optical accessibility to study the ignition and combustion process of classical pre-chamber jet ignition.

### 1.2 Flame accelerated ignition

Relatively slow combustion velocity is one of the bottlenecks which limits the thermal efficiency of SI engines. Therefore, increased flame speed is required to improve the combustion characteristics of SI engines. In fundamental research field on combustion, the phenomenon of flame acceleration has been widely studied. It was found that the

flame would be accelerated while travelling in either a smooth or an obstructed tunnel. The phenomenon results from the effect of gas flow and turbulence [15]. However, flame acceleration is more obvious in an obstructed tunnel because the obstacles are effective to enhance the gas flow and increase the flame surface [16]. As a result, the flame can be suddenly accelerated when passing by the obstacles [17].

Flame acceleration inside a tunnel is an attractive phenomenon but rarely associate with automotive piston engines. However, the phenomenon exactly meets the demand of improving combustion characteristics for SI engines. Therefore, a new ignition mode which combines the concept of flame acceleration in tunnel and pre-chamber jet ignition was proposed by the authors, called Flame Acceleration Ignition (FAI) [18]. An FAI system is composed of a spark plug and a flame acceleration tunnel with small dimensions. The spark plug is set on one side of the tunnel and the other side is connected with the main combustion chamber. Obstacles are set inside the tunnel to achieve better acceleration effect in a relatively short tunnel. Considering that annulus is the most common and classical shape for the obstacles in flame acceleration researches, it was selected for the experiments in this paper. In general, the FAI system occupies a small proportion of the combustion volume so that it can be regarded as a pre-chamber. However, the exit of the FAI system is widely opened, which is different from classical pre-chamber designs characterized by relatively small nozzle dimensions.

In FAI mode, the flame kernel is formed by the spark plug on the top end and then the flame is accelerated through the tunnel. Subsequently, the mixture in the main chamber can be rapidly ignited by the flame jet rushed out of the tunnel. Therefore, the combustion in the main chamber can be enhanced and accelerated, which is beneficial to improving the thermal efficiency.

## 2 Experimental Setups

### 2.1 Rapid compression machine

In this study, Tsinghua University Rapid Compression Machine (TU RCM) [19] was utilized to study the combustion process of both classical pre-chamber jet ignition and flame accelerated ignition. TU RCM consists of high pressure gas tank, driver section, hydraulic section, compression section, and combustion chamber. The compression stroke and combustion chamber bore are 495 mm and 50.8 mm, respectively. The compression ratio is adjustable by varying the length of combustion chamber. In this study, the compression ratio was fixed at 9.5.

At the end of combustion chamber, the metal cover can be replaced by the quartz window with the same bore as the chamber to provide optical access. High speed photography was accomplished by camera Photron SA-X2 coupled with a 180 mm lens Nikon AF Micro f/4D, which was set in the axial direction to record the combustion images. The f3.5 aperture was chosen. The shutter time and the frame rate were set as 1/12661 s and 12500 fps, respectively. Each image had an original resolution of 896\*896 and was processed to a circular shape with the diameter of 700 pixels, corresponding to the range of the combustion chamber.

The pre-chamber jet ignition system was set on the circumferential edge of the combustion chamber. A hemispherical design was used for the classical pre-chamber jet ignition investigation, which is shown in Figure 1(a). The pre-chamber occupied 1.25% of the total combustion volume, multiple nozzle configurations were tested. As shown in Figure 1(b), in FAI experiments, a 3-obstacle FAI system was used. The length and the diameter of the tunnel were 27 mm and 7 mm, respectively. The blockage ratio of

the annular obstacles was 0.36, i.e. the cross-section diameter of the obstacles was 80% of that of the tunnel. Note that the FAI system did not occupy the original combustion volume, there would be slight reduction in compression ratio (9.4).

As shown in Figure 1, a pressure sensor Kistler 6125C was set on the opposite side of the ignition system, measuring the pressure inside the main chamber at a sampling rate of 100 kHz. To transform the signal to the voltage version, a charge amplifier Kistler 5018A was used.

Synchronous trigger signal was produced by a pulse generator DG645. The TTL trigger signal would be generated within 2 ms after the piston reached the top dead center, according to the in-cylinder pressure. Therefore, the spark plug and the high-speed camera could action at the same time when zero time ( $t=0$ ) was marked. Both pressure signal and trigger signal were acquired by National Instrument chassis cDAQ-9178 and analog input module cDAQ-9223.

The mixture of methane, oxygen and nitrogen was used in this study. Methane is the major component of natural gas. Oxygen and nitrogen were used to simulate air. Stoichiometric combustion condition was investigated so that the volumetric ratio between methane, oxygen and nitrogen was 1:2:7.52. The mixture was prepared according to Dalton's Law of Partial Pressure.

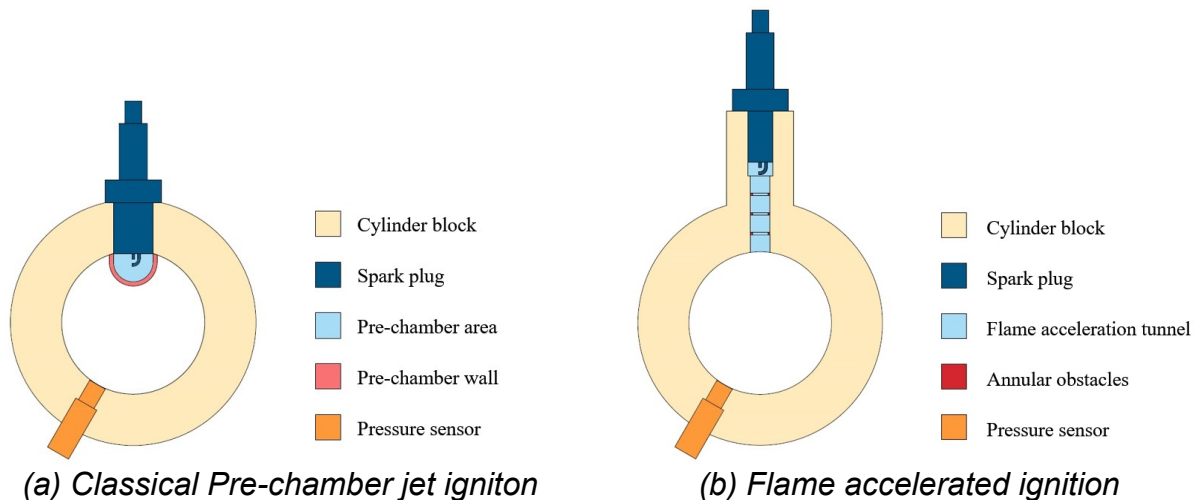


Figure 1: Cross-section view of the RCM combustion chamber

## 2.2 Natural gas engine

In this study, FAI was further tested in a single cylinder natural gas engine with the displacement of 1.85 L after the RCM experiments. The original compression ratio of the engine was 10.5. A dynamometer Horiba LI250 was connected to the engine. The natural gas was port injected at a pressure of 0.5 MPa. The intake air was controlled by a 6-channel sonic nozzle system. A pressure sensor AVL GU22C coupled with a charge amplifier Kistler 5011 was used to measure the in-cylinder pressure. Moreover, engine control, online combustion analysis and high-speed data acquisition were conducted by a LabVIEW system composed of National Instrument real-time system, FPGA and driven modules.

Figure 2 shows the schematic of the engine assembled with an FAI system. Compared with the original engine, the position of spark plug assembly was replaced by the FAI system. Detailed configuration of FAI systems will be discussed in Results and Discussions. The compression ratio would be reduced due to the introduction of the extra

combustion space. However, considering that the volume occupied by flame acceleration tunnel was very little in comparison with the main chamber, in this study, the compression ratio was still no lower than 10.4 in FAI mode.

During the experiment, the engine speed was fixed at 1000 r/min. And the engine was operated at the load with the indicated mean effective pressure (IMEP) of 0.65 MPa. Combustion with different mixture condition (excess air ratio,  $\lambda$ ) was conducted to compare the performance and characteristics of FAI mode and conventional spark ignition (CSI) mode.

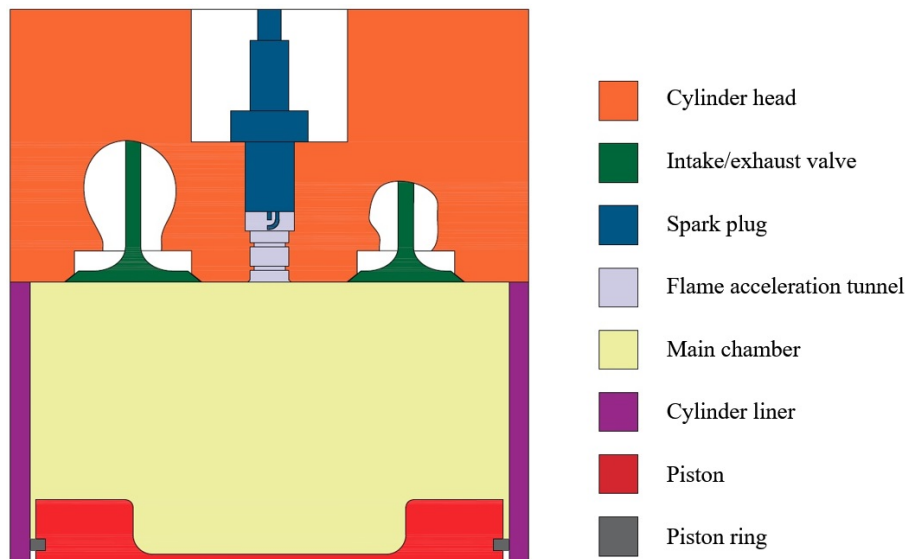


Figure 2: Schematic of the engine assembled with FAI system

### 3 Results and Discussions

#### 3.1 Classical pre-chamber jet ignition investigations on RCM

Firstly, a series of 4-nozzle classical pre-chamber designs were chosen for the RCM experiments. The nozzles are symmetrically distributed. And the angle between the axis of each nozzle and the centerline of the pre-chamber was fixed at  $45^\circ$ . The sole difference between the designs was the nozzle size. The diameter of the nozzles varied from 1.0 mm to 2.0 mm.

Figure 3 shows the pressure inside the main chamber of each designs. Conventional spark ignition case is also shown for comparison. It can be seen that all of 5 pre-chamber jet ignition cases have remarkably earlier pressure increase in comparison to CSI case, indicating that the combustion is effectively accelerated and enhanced by utilizing pre-chamber jet ignition. Pre-chamber jet ignition cases with the nozzle diameter of 1.1 mm, 1.2 mm, 1.6 mm, and 2.0 mm show similar pressure characteristic. The pressure rise of  $4 \times \Phi 1.2$  mm case is slightly faster and that of  $4 \times \Phi 2.0$  mm case is slightly slower than others. However,  $4 \times \Phi 1.0$  mm case appears disparate combustion pressure trace. The pressure inside the main chamber keeps nearly unchanged for quite a long time after discharge of the spark plug. During this period, the pressure is even lower than that of the CSI case, indicating that the combustion inside the main chamber does not initiate. However, the pressure of the main chamber starts to rapidly

rise with a higher slope after the lag, which means the  $4\times\Phi 1.0$  mm case possesses the fastest combustion duration in the main chamber among all tested cases. There is little difference of nozzle size between  $4\times\Phi 1.0$  mm case and  $4\times\Phi 1.1$  mm case. However, the disparity of combustion pressure is significant. To analyze the cause, the partial enlarged pressure traces of the main chamber, together with corresponding heat release rates and their derivate are shown in Figure 4. Both pressure traces decrease slightly in  $0\sim 1.8$  ms due to the wall heat transfer and turn to increase then. However, the degree of increase is rather different. The main chamber pressure of  $4\times\Phi 1.1$  mm case appears sharp increase, corresponding to obvious heat release. It can be inferred that the combustion inside the main chamber is initiated since  $t=1.8$  ms. In contrast, for  $4\times\Phi 1.0$  mm case, the increase amplitude is only 0.01 MPa and the increase trend terminates at  $t=3.8$  ms. During this period, the heat release is tiny. It is apparent that the slight increase of main chamber pressure results from the combustion inside the pre-chamber. Some of the hot gas enters the main chamber through nozzles driven by the pressure difference, which slightly boosts the pressure inside the main chamber. With the end of pre-chamber combustion, the pressure inside the main chamber turns to decrease without any heat release. At  $t=4.4$  ms, the pressure begins to rise again, which marks the initiation of the combustion in the main chamber. Therefore, in  $4\times\Phi 1.1$  mm case, the combustion inside the pre-chamber and the main chamber is continuous. While in  $4\times\Phi 1.0$  mm case, the combustion in the two chambers is obviously interrupted. In this paper, the former one is called single stage combustion mode and the latter one is called double stage combustion mode. Heat release rate and its derivate can be used as the criterion to distinguish the combustion mode. Single stage mode is characterized by monotonicity of the combustion pressure increase and the heat release rate increase. However, double stage mode does not possess the feature. Therefore, once the derivate of the heat release rate appears negative, the combustion can be determined as the double stage mode.

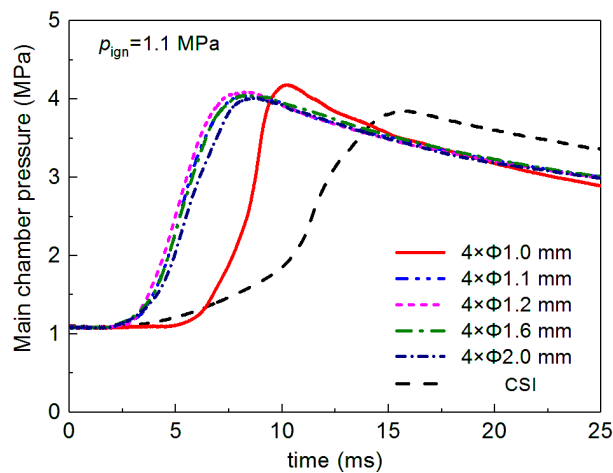


Figure 3: Main chamber pressure of pre-chamber jet ignition with different nozzle size (1.1 MPa at spark timing)

## 8.2 Experimental Research on Pre-chamber Jet Ignition in Rapid Compression Machine and Natural Gas Engine

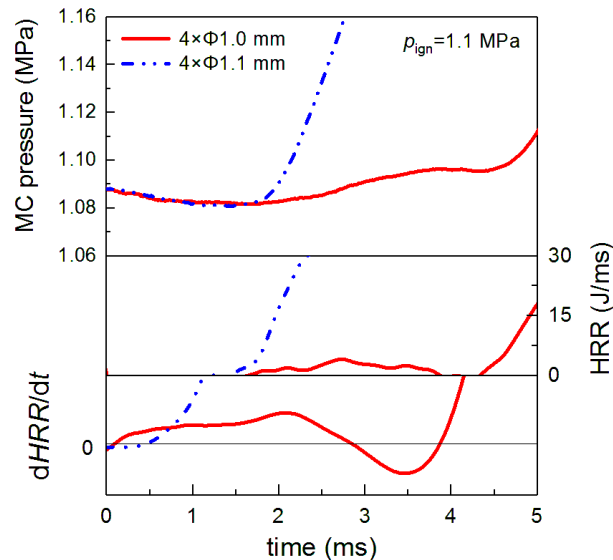


Figure 4: comparison of main-chamber pressures, heat release rates and their derivative of  $4 \times \Phi 1.0$  mm case and  $4 \times \Phi 1.1$  mm case (1.1 MPa at spark timing)

Figure 5 shows the ignition delay (defined as the time interval between spark and 10% heat release) and the combustion duration (defined as the time interval between 10% heat release and 90% heat release) of tested cases. It can be clearly found that the ignition delay and the combustion duration among all single stage combusted pre-chamber jet ignition cases are respectively similar, although the total cross-sectional area of nozzles was tripled from the  $4 \times \Phi 1.1$  mm case to the  $4 \times \Phi 2.0$  mm case. Compared with the CSI case, the ignition delay and combustion duration of single stage combusted pre-chamber jet ignition are shortened by 45% and 55%, respectively. Double stage combusted pre-chamber jet ignition (i.e.  $4 \times \Phi 1.0$  mm case) shows different characteristics on combustion parameters. The ignition delay is obviously longer than that of single stage mode and even comparable to that of CSI due to the lag of the second stage combustion. However, the combustion duration of double stage mode is manifestly shorter than that of any other cases.

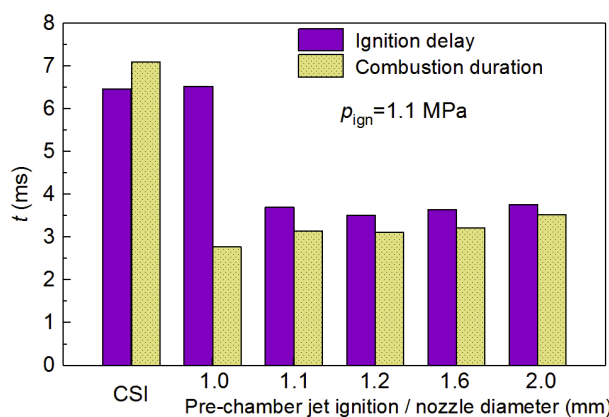


Figure 5: ignition delay and combustion duration of tested cases (1.1 MPa at spark timing)

Except for 4-nozzle cases, multiple pre-chamber configurations including single-nozzle designs and double-nozzle designs with various diameter were tested. The results are shown in Figure 6. It can be concluded that misfire occurs in the main chamber when

the nozzle dimension is below a certain threshold. With the increase of nozzle dimension, the mixture inside the main chamber could be indirectly ignited by the jet and the combustion is double-staged. However, the range of nozzle configuration led to double stage combustion is limited. As the nozzles are further enlarged, the combustion transforms to the single stage mode. It can be also found in Figure 6 that total cross-sectional area of nozzles is not the exclusive factor which affect the combustion mode at a certain pressure and temperature condition. Besides, the number of nozzles is also a minor factor because the increase of the nozzle number means the increase of contact surface area between the jets and the nozzle walls, resulting in more heat transfer.

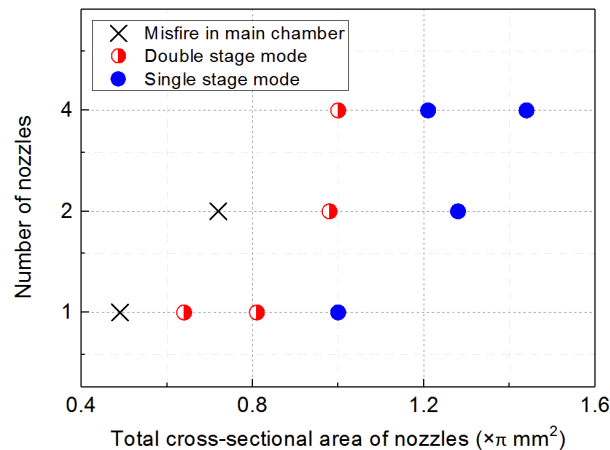


Figure 6: relationship between nozzle configuration and combustion mode (1.1 MPa at spark timing)

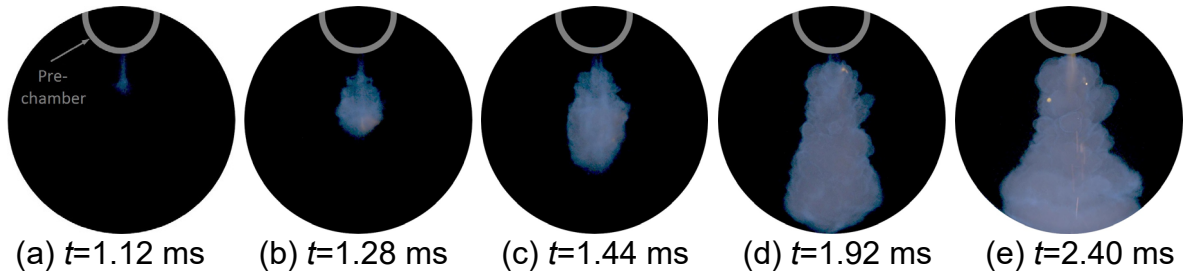
Figure 7 and Figure 8 display the ignition and combustion process (the contrast of images is improved) in the main chamber of single stage mode and double stage mode, respectively, corresponding to single-nozzle designs with the diameter of 3.0 mm (1 $\times\Phi$ 3.0 mm case) and 1.6 mm (1 $\times\Phi$ 1.6 mm case).

According to Figure 7, in the single stage case, the flame jet first appears in the main chamber at 1.12 ms after spark, indicating that the combustion inside the pre-chamber has already finished at that time. The flame jet generates from the nozzle and develops rapidly through the main chamber until it reaches the opposite side at approximately 2 ms. It means that the flame jet penetrates the main chamber in less than 1 ms. It can be calculated that the average propagation speed along the axial direction of the jet is over 50 m/s, exceeding 15 times than that of conventional flame propagation (approx. 3 m/s at the same condition). During the developing process, the flame is composed of thin fire near the nozzle and approximately conical fire in the tip.

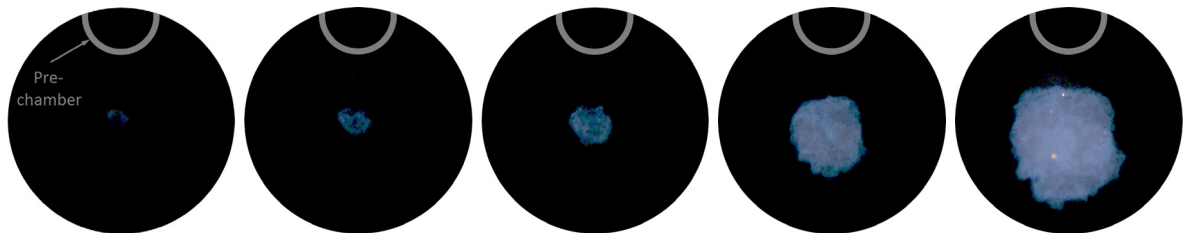
As shown in Figure 8, in the double stage case, there is not any visible flame until 6.40 ms after spark. Compared with synchronous phenomenon of single stage mode, it can be concluded that the flame is quenched through the small dimension nozzle. The intense heat transfer cools the jet formed in the main chamber which cannot ignite the mixture directly. However, the jet composed of combusted and intermediate products still possess appropriate temperature to drive low temperature reaction, resulting in the ignition after a period of lag time. It can be clearly observed that the ignition occurs in the position far away from the nozzle, which is absolutely different from the single stage mode. Moreover, the flame develops evenly along each direction, with a high speed near 100 m/s. As a result, the 2D projection of the flame keeps approximately circular throughout the combustion process. It can be inferred that the jet preheats the mixture



and improve the reactivity in the main chamber during the lag period so that the following combustion is markedly enhanced.



(a)  $t=1.12$  ms    (b)  $t=1.28$  ms    (c)  $t=1.44$  ms    (d)  $t=1.92$  ms    (e)  $t=2.40$  ms  
 Figure 7: ignition and combustion process in main chamber of single stage mode ( $1 \times \Phi 3.0$  mm case, 1.4 MPa at spark timing, contrast improved)



(a)  $t=6.40$  ms    (b)  $t=6.56$  ms    (c)  $t=6.72$  ms    (d)  $t=7.20$  ms    (e)  $t=7.68$  ms  
 Figure 8: ignition and combustion process in main chamber of double stage mode ( $1 \times \Phi 1.6$  mm case, 1.4 MPa at spark timing, contrast improved)

Figure 9 and Figure 10 display the repeated test results of a single stage case and a double stage case, respectively. Pressure traces of single stage combustion appear good repeatability. On the contrary, those of double stage mode are dispersed. In double stage mode, the ignition inside the main chamber has relatively high randomness, leading to instability of ignition delay and combustion phase, which is unsatisfying in engine applications.

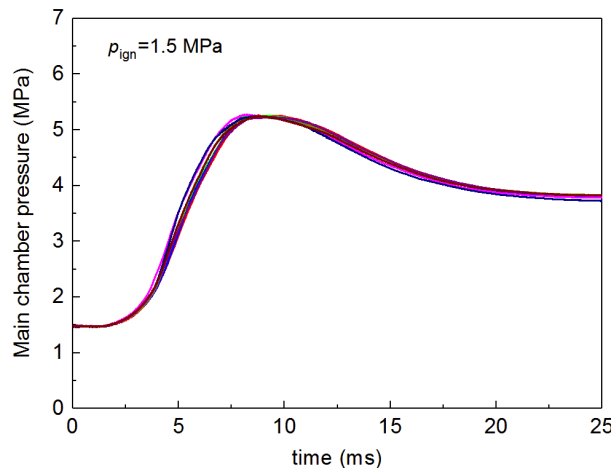


Figure 9: repeated test results of a single stage case

## 8.2 Experimental Research on Pre-chamber Jet Ignition in Rapid Compression Machine and Natural Gas Engine

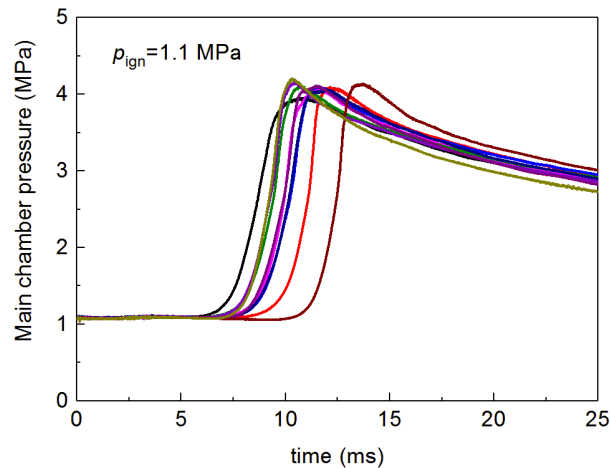


Figure 10: repeated test results of a double stage case

### 3.2 Flame acceleration ignition investigations on RCM and natural gas engine

Figure 11 shows the comparison of in-cylinder pressure and heat release rate between FAI and CSI in RCM. The effect of accelerating combustion process achieved by FAI can be apparently recognized. Compared with CSI, the heat release peak of FAI comes 10 ms earlier with 20% higher value. The combustion process can be shortened by 40%, indicating the potential to improve combustion characteristics of SI engines.

Figure 12 records the combustion process (the contrast and brightness of images are improved) in the main chamber of FAI. The flame is generated and accelerates inside the tunnel until 1.92 ms after spark when it rushes into the main chamber (see Figure 12(a)). And then the flame curls outwards near the tunnel exit soon (see Figure 12(b)) which extends the radial width of the flame jet. After the initial period, the flame develops mainly along the axial direction at an average speed over 20 m/s. During the process, the flame jet maintains nearly cylindrical, igniting the surrounding mixture. As a result, the radial dimension of the flame also keeps growing at a speed faster than conventional flame propagation.

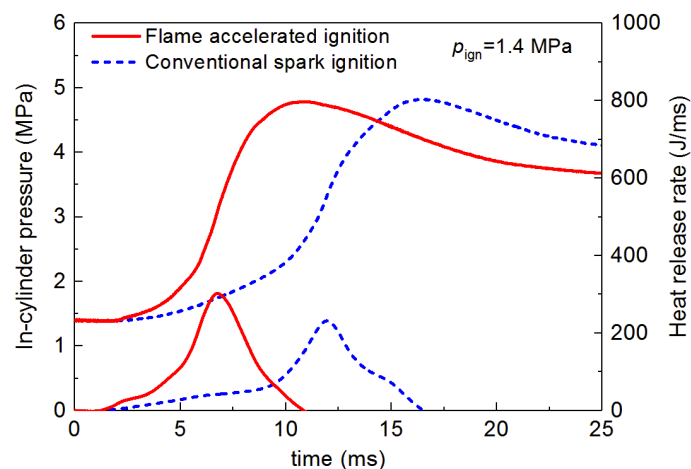
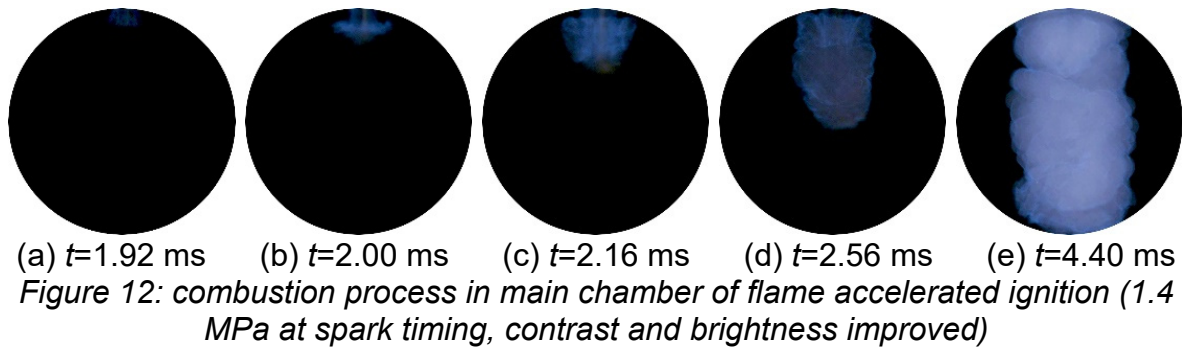


Figure 11: comparison of in-cylinder pressure and heat release rate between FAI and CSI in RCM (1.4 MPa at spark timing)

## 8.2 Experimental Research on Pre-chamber Jet Ignition in Rapid Compression Machine and Natural Gas Engine



The RCM experiments indicated that the combustion could be evidently enhanced by FAI. On this basis, FAI is further tested in the natural gas engine. A 2-obstacle FAI system was assembled. The length and the diameter of the tunnel were 14 mm and 10 mm, respectively. The blockage ratio of the annular obstacles was 0.36, which was the same as that in RCM experiment.

Figure 13 shows the in-cylinder pressure and heat release rate of FAI under different mixture conditions. Corresponding CSI cases are also included for comparison. After spark, the response of pressure rise induced by FAI is slower than that of CSI, which means the heat release of FAI acts later. However, the heat release rate of FAI boosts to an evidently higher level subsequently, indicating that FAI induced combustion is faster and more centralized. Both cases with different mixture condition displayed in Figure 13 follow the characteristic. But the advantage of enhancing combustion is weakened with the introduction of excess air.

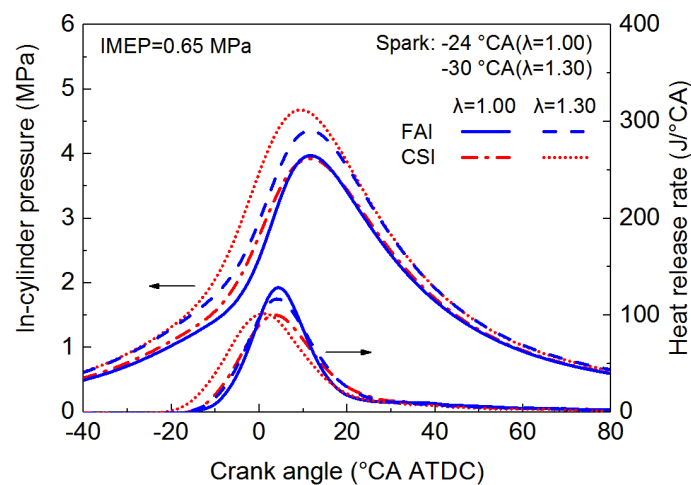


Figure 13: In-cylinder pressure and heat release rate of FAI in engine, compared with CSI

Figure 14 compares the ignition delay between FAI and CSI under different conditions. During the experiment, the spark timing was swept in order to cover the maximum output point. It can be primarily found from Figure 14 that misfire occurs in FAI mode when spark takes place at a relative early timing. It is clear that there is residual gas trapped in the tunnel after a combusted cycle. The fresh mixture has not been fully compressed into the tunnel to form an ignitable atmosphere in the position of spark plug at the early timing, resulting in misfire. With the increase of lean level, the range of optional spark timing becomes narrower.

The difference of ignition delay between FAI and CSI is notable that the former one is obviously longer than the latter one. In lean-burn conditions, the gap is further widened.

The characteristic can be ascribed to the adverse mixture atmosphere caused by residual gas inside the tunnel in FAI mode. With the addition of excess air, the natural gas concentration at spark position is further reduced, which prolongs the process of flame kernel formation and its initial development.

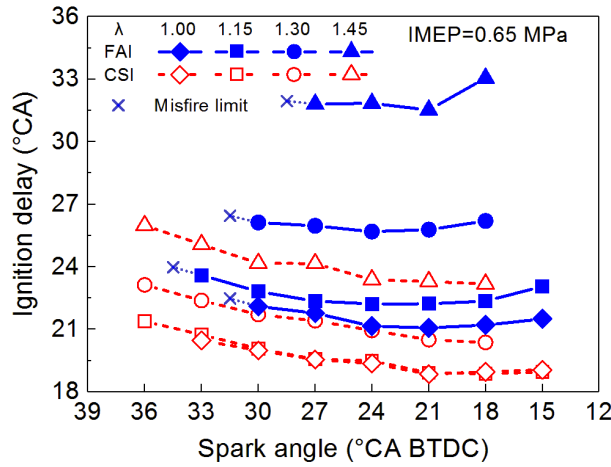


Figure 14: comparison of ignition delay between FAI and CSI

Figure 15 displays the CA10-CA50 duration. FAI mode shows advantage in this parameter when  $\lambda$  is less than 1.45. The effect of enhancing combustion by FAI can be directly proved according to the characteristic. FAI possesses the capacity to accelerate the first-half combustion. More importantly, the process of first-half combustion takes place around the top dead center, where the impact of heat release on the thermal efficiency is quite sensitive and significant. Hence, the feature of FAI is beneficial to improving the thermal efficiency. However, as  $\lambda$  increases, the advantage on CA10-CA50 fades gradually. When  $\lambda$  reaches 1.45, the benefit no longer exists at late spark timing.

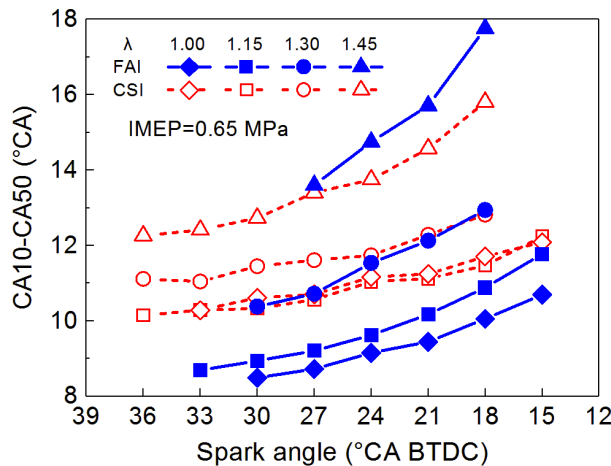


Figure 15: comparison of CA10-CA50 duration between FAI and CSI

CA50 is shown in Figure 16, which is the comprehensive result of ignition delay and CA10-CA50 duration. When the combustion takes place at stoichiometric condition or lean-burn condition with relative low  $\lambda$  ( $\leq 1.15$ ), the CA50 of FAI is comparable to that of CSI, because the accelerated CA10-CA50 duration of FAI erases the difference of ignition delay between two modes, which means that FAI possesses the capacity to

realize similar CA50 with less negative work at certain mixture conditions. Nevertheless, as the mixture becomes much leaner, the difference of CA50 between two modes gets larger as the advantage of CA10-CA50 duration achieved by FAI is narrowed while the disadvantage of ignition delay is sharply widened. Under the circumstance, the spark timing has to be advanced to adjust the combustion phase. However, the optional spark timing is limited by misfire.

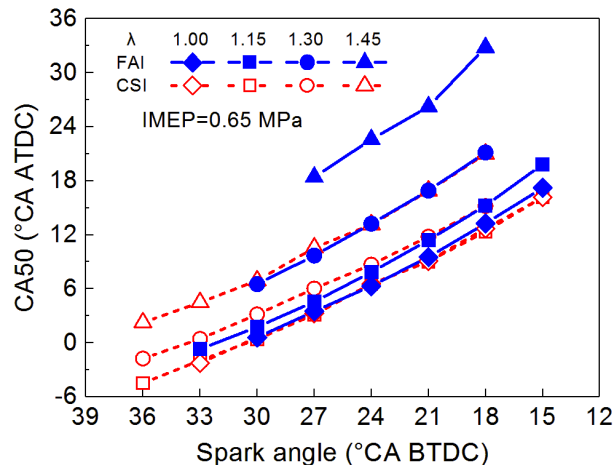


Figure 16: comparison of CA50 between FAI and CSI

Figure 17 compares the indicated thermal efficiency (ITE) of FAI and CSI under different conditions. FAI achieves higher efficiency than CSI due to the beneficial of reduced negative work and accelerated combustion process except for  $\lambda=1.45$  condition. The best ITE improves 0.6, 0.5 and 0.2 percent when  $\lambda$  is 1.00, 1.15 and 1.30, respectively. It is clear that the biggest advantage of FAI appears at stoichiometric condition. For  $\lambda=1.45$  condition, the suitable combustion phase cannot be attained which is restricted by misfire, resulting in unsatisfying ITE.

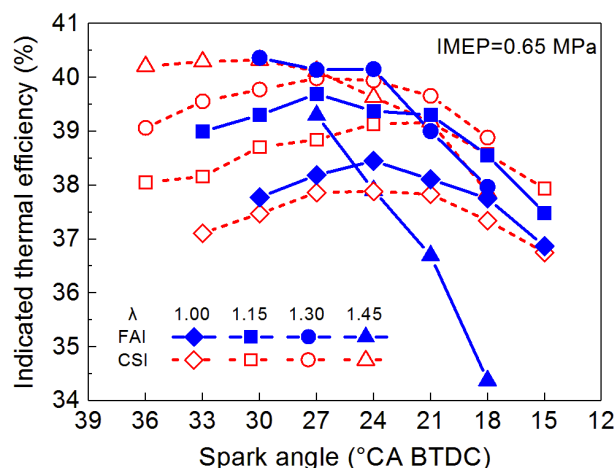


Figure 17: comparison of indicated thermal efficiency between FAI and CSI

Combustion stability is compared in Figure 18 using the coefficient of variation (COV) calculated by IMEP of consecutive cycles. Except for the leanest condition, the COV is comparable and all of them is under 3%. However, the COV of FAI under  $\lambda=1.45$  condition is unacceptably high, reflecting that the stability of FAI with lean combustion needs to be improved.

## 8.2 Experimental Research on Pre-chamber Jet Ignition in Rapid Compression Machine and Natural Gas Engine

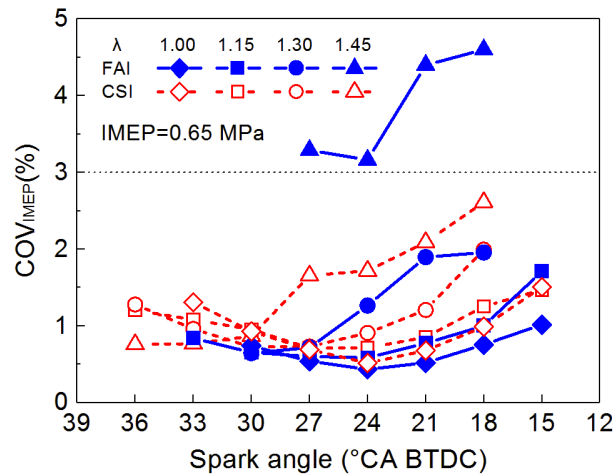


Figure 18: comparison of coefficient of variation between FAI and CSI

It can be concluded from the above engine test results that the performance of FAI under lean-burn condition is limited by misfire due to residual gas trapped in the tunnel. In order to solve the problem, the FAI system is modified by introducing a space by the side of spark position, named residual gas cavity, as shown in Figure 19. The residual gas cavity is off-centered, serving for storage of the residual gas. During the compression stroke, the residual gas which has not been exchanged outside the tunnel will be compressed to the cavity space instead of remained at the spark position in the effect of piston motion. Thus the ignition inside the tunnel can be ensured. The tunnel length and diameter of the modified design were 15 mm and 6 mm, respectively. The number and blockage ratio of the annular obstacles were kept the same with the original design.

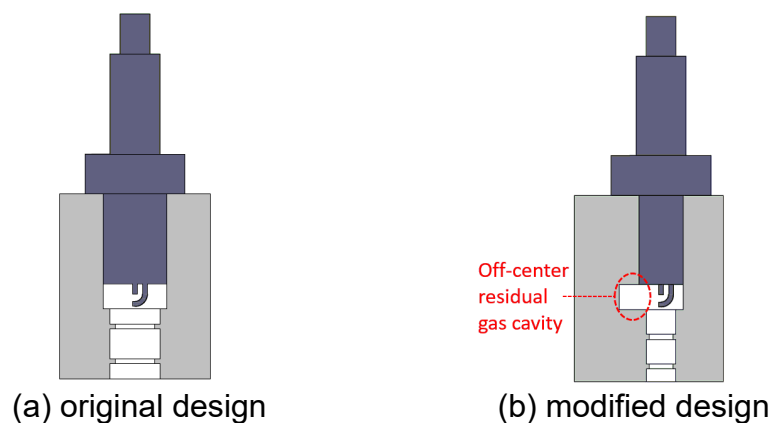


Figure 19: the original design and modified design (with residual gas cavity) of FAI system assembled in the engine

Figure 20 shows the in-cylinder pressure and heat release rate of modified FAI. The characteristics of late pressure response and centralized heat release remain. Ignition delay is shown in Figure 21. Although FAI still behaves longer ignition delay, the gap is effectively narrowed, indicating that the ignition and combustion process inside the tunnel is improved. More importantly, attributing to the introduction of residual gas cavity, misfire limit has been eliminated which provides the capacity to adjust combustion phase flexibly.

The indicated thermal efficiency and coefficient of variation are displayed in Figure 22 and Figure 23, respectively. On account of above improvement, modified FAI gains higher ITE than CSI with acceptable combustion stability under all mixture conditions.

As a result, the lean-burned FAI performance is effectively enhanced by the modification with residual gas cavity.

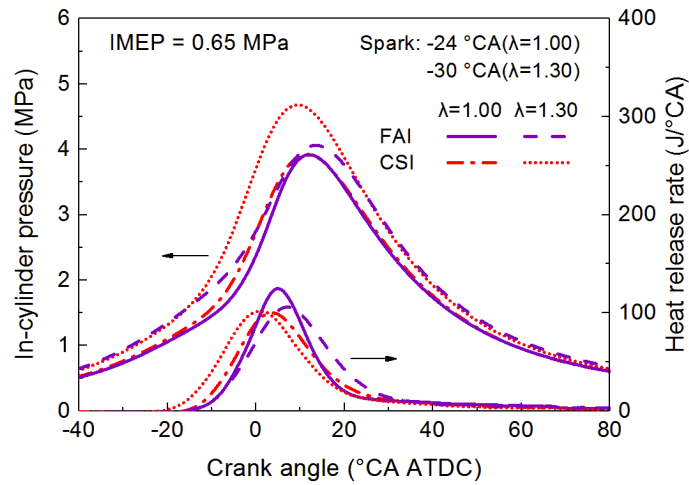


Figure 20: In-cylinder pressure and heat release rate of modified FAI with residual gas cavity in engine, compared with CSI

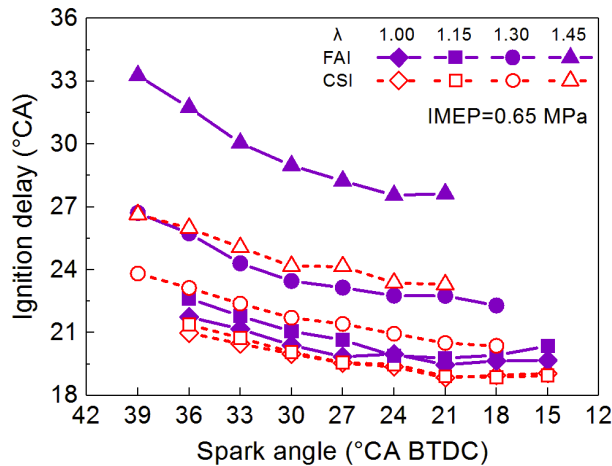


Figure 21: comparison of ignition delay between modified FAI with residual gas cavity and CSI

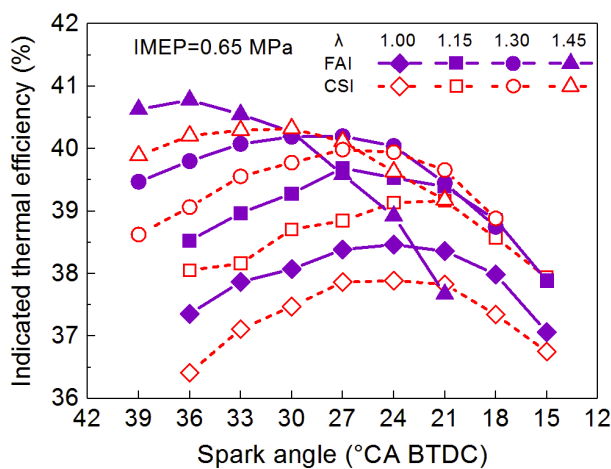


Figure 22: comparison of indicated thermal efficiency between modified FAI with residual gas cavity and CSI



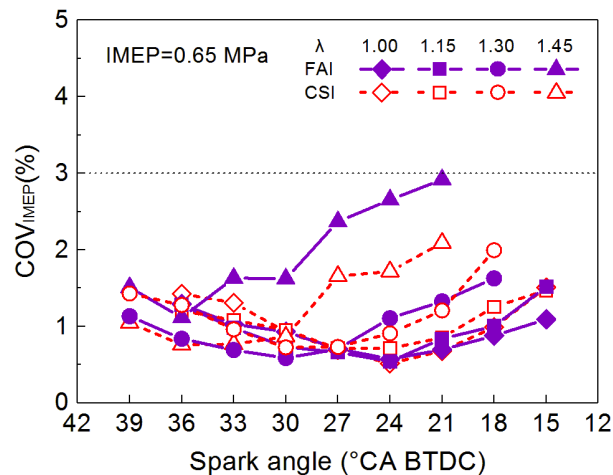


Figure 23: comparison of coefficient of variation between modified FAI with residual gas cavity and CSI

## 4 Conclusions

In this paper, classical pre-chamber jet ignition and a new pre-chamber jet ignition method called flame accelerated ignition were investigated. Optical RCM was used to detailed study the ignition and combustion process of both methods. Moreover, the newly proposed flame accelerated ignition was tested in a single cylinder natural gas engine. The conclusions are summarized as following:

- (1) The classical pre-chamber jet ignition is classified as two modes: double stage combustion and single stage combustion. Under a certain pressure and temperature condition, nozzle configuration is the key factor affecting the combustion mode.
- (2) Double stage combustion mode takes place in the condition with relatively small nozzle dimension. The jet cannot ignite the mixture in the main chamber directly due to the quenching effect. Ignition inside the main chamber occurs away from the nozzle after a lag time, initiating the speedy second-stage combustion. Therefore, double stage combustion shows long ignition delay and extremely short combustion duration. Due to the randomness of ignition in the main chamber, the combustion stability of double stage mode is unsatisfying. Moreover, the range of nozzle configuration led to double stage combustion is narrow.
- (3) With the increase of nozzle dimension, combustion switches to the single stage mode. The mixture in the main chamber is directly ignited by the flame jet developing from the nozzle. Hence the combustion inside the pre-chamber and the main chamber takes place continuously, showing single-stage characteristic. In this mode, the ignition delay and the combustion duration can be shortened simultaneously with satisfying combustion stability. The flame jet consists of thin fire near the nozzle and approximately conical fire in the tip, expanding rapidly with axial speed over 15 times than that of conventional flame propagation.
- (4) According to the concept of flame acceleration in tunnel and pre-chamber jet ignition, flame accelerated ignition is realized by a flame acceleration tunnel set between the spark plug and the main chamber. RCM experiment proved the effect of enhancing combustion achieved by FAI. The mixtures in the main chamber can be rapidly ignited by the cylindrical flame jet rushed out of the tunnel.



- (5) According to the engine test results, FAI possesses the capacity to reduce negative work and accelerate combustion, leading to higher thermal efficiency than conventional spark ignition. The best performance takes place at stoichiometric condition. With the increase of excess air ratio, the advantages are weakened and the combustion phase is restricted by misfire due to the residual gas trapped in the tunnel. The introduction of residual gas cavity eliminates the misfire and guarantees the performance of FAI under all mixture conditions.

### Literatures:

- [1] Toulson E, Schock H J, Attard W P. A review of pre-chamber initiated jet ignition combustion systems[J]. SAE Technical Paper 2010-01-2263, 2010.
- [2] Shah A, Tunestal P, Johansson B. Investigation of performance and emission characteristics of a heavy duty natural gas engine operated with pre-chamber spark plug and dilution with excess air and EGR[J]. SAE International Journal of Engines, 2012, 5(4):1790-1801.
- [3] Takashima Y, Tanaka H, Sako T, et al. Evaluation of engine performance and combustion in natural gas engine with pre-chamber plug under lean burn conditions[J]. SAE International Journal of Engines, 2014, 8(1):221-229.
- [4] Attard W P, Blaxill H, Anderson E K, et al. Knock limit extension with a gasoline fueled pre-chamber jet igniter in a modern vehicle powertrain[J]. SAE International Journal of Engines, 2012, 5(3):1201-1215.
- [5] Anderson E K, Attard W P, Brown A, et al. Experimental study of a pre-chamber jet igniter in a turbocharged rotax 914 aircraft engine[J]. SAE Technical Paper 2013-01-1629, 2013.
- [6] Attard W P, Fraser N, Parsons P, et al. A turbulent jet ignition pre-chamber combustion system for large fuel economy improvements in a modern vehicle powertrain[J]. SAE International Journal of Engines, 2010, 3(2):20-37.
- [7] Shah A, Tunestal P, Johansson B. Effect of relative mixture strength on performance of divided chamber 'avalanche activated combustion' ignition technique in a heavy duty natural gas engine[J]. SAE Technical Paper 2014-01-1327, 2014.
- [8] Gentz G, Thelen B, Litke P, et al. Combustion visualization, performance, and cfd modeling of a pre-chamber turbulent jet ignition system in a rapid compression machine[J]. SAE International Journal of Engines, 2015, 8(2):538-546.
- [9] Thelen B C, Gentz G, Toulson E. Computational study of a turbulent jet ignition system for lean burn operation in a rapid compression machine[J]. SAE Technical Paper 2015-01-0396, 2015.
- [10] Gentz G, Thelen B, Gholamisheeri M, et al. A study of the influence of orifice diameter on a turbulent jet ignition system through combustion visualization and

- performance characterization in a rapid compression machine[J]. *Applied Thermal Engineering*, 2015, 81:399-411.
- [11] Gentz G, Gholamisheeri M, Toulson E. A study of a turbulent jet ignition system fueled with iso-octane: Pressure trace analysis and combustion visualization[J]. *Applied Energy*, 2017, 189:385-394.
- [12] Gholamisheeri M, Thelen B C, Gentz G R, et al. Rapid compression machine study of a premixed, variable inlet density and flow rate, confined turbulent jet[J]. *Combustion and Flame*, 2016, 169:321-332.
- [13] Thelen B C, Toulson E. A computational study of the effects of spark location on the performance of a turbulent jet ignition system[J]. *SAE Technical Paper 2016-01-0608*, 2016.
- [14] Validi A A, Schock H, Jaber F. Turbulent jet ignition assisted combustion in a rapid compression machine[J]. *Combustion and Flame*, 2017, 186:65-82.
- [15] Dorofeev S B. Hydrogen flames in tubes: Critical run-up distances[J]. *International Journal of Hydrogen Energy*, 2009, 34(14):5832-5837.
- [16] Silvestrini M, Genova B, Parisi G, et al. Flame acceleration and DDT run-up distance for smooth and obstacles filled tubes[J]. *Journal of Loss Prevention in the Process Industries*, 2008, 21(5):555-562.
- [17] Ciccarelli G, Dorofeev S. Flame acceleration and transition to detonation in ducts[J]. *Progress in Energy & Combustion Science*, 2008, 34(4):499-550.
- [18] Wang B, Wang Z, Liu C, et al. Experimental study of flame accelerated ignition on rapid compression machine and heavy duty engine[J]. *SAE Technical Paper 2017-01-2242*, 2017.
- [19] Di H, He X, Zhang P, et al. Effects of buffer gas composition on low temperature ignition of iso-octane and n-heptane[J]. *Combustion and Flame*, 2014, 161(10):2531–2538.